

Photoresponse of organic field-effect transistors based on conjugated polymer/fullerene blends

N. Marjanović^{a,*}, Th.B. Singh^a, G. Dennler^a, S. Günes^a, H. Neugebauer^a,
N.S. Sariciftci^a, R. Schwödjaer^b, S. Bauer^b

^a Linz Institute for Organic Solar Cells (LIOS), Physical Chemistry, Johannes Kepler University Linz, Altenbergerstrasse 69, Linz, A-4040, Austria

^b Soft Matter Physics, Johannes Kepler University Linz, Altenbergerstrasse 69, Linz, A-4040, Austria

Received 22 November 2005; accepted 9 January 2006

Available online 7 February 2006

Abstract

Results on photoresponsive organic field-effect transistors (photOFETs) based on conjugated polymer/fullerene solid-state mixtures as active semiconductor layer and poly-vinyl-alcohol (PVA) or divinyltetramethyldisiloxane-bis(benzocyclobutene) (BCB) as gate dielectrics are presented. With LiF/Al top source–drain contacts all devices show dominantly n-type transistor behaviour. Devices fabricated with PVA as gate insulator reveal gate voltage induced saturation upon illumination but low photostability. Contrary, devices fabricated with BCB as gate insulator show transistor amplification in a wide range of illumination intensities. The increase of the drain–source current by more than two orders of magnitudes upon illumination is explained by the generation of a large carrier concentration due to photoinduced charge transfer at the conjugated polymer/fullerene bulk heterojunction upon illumination (photodoping). After illumination, a change of the dark transfer characteristics with respect to the initial transfer characteristics was observed. The initial dark state is achieved either by applying a large negative gate bias or by annealing.

© 2006 Elsevier B.V. All rights reserved.

PACS: 85.60.Dw; 85.30.Tv

Keywords: Phototransistors; Organic field-effect transistors (OFETs); Organic dielectrics; Conjugated polymer/fullerene bulk heterojunction

1. Introduction

Organic field-effect transistors (OFETs) play a prominent role in organic semiconductor based elec-

tronic devices due to the possibility of switching and driving thin film transistors (TFT) in flexible displays, smart cards, radio frequency identification (RFID) tags and large area sensor arrays [1–3]. An advantage of organic devices is the capability of being processed from solution allowing low cost/large scale fabrication techniques, such as ink-dot printing [4]. Light emitting diodes and

* Corresponding author. Tel.: +43 732 2468 8767; fax: +43 732 2468 8770.

E-mail address: nenad.marjanovic@jku.at (N. Marjanović).

displays based on organic semiconductors are already entering the market. Organic solar cells have reached efficiencies exceeding 4% [5a,b]. OFETs with mobilities up to $1 \text{ cm}^2/\text{V s}$ are investigated in academic as well as in industrial laboratories catching up fast with the performance of amorphous silicon TFT devices [6a,b].

Photoresponsivity of organic field-effect transistors (photOFETs) is interesting since it is the basis for light sensitive transistors. PhotOFETs can be used e.g. for light induced switches, light triggered amplification, detection circuits and, in photOFET arrays, for highly sensitive image sensors. The realisation of photoactive organic field-effect transistors has been demonstrated using various organic and polymeric semiconductors. Responsivity as high as 0.5–1 A/W has been achieved using pristine poly(3-octylthiophene) [7], polyfluorene [8], bifunctional spiro compounds [9] and polyphenyleneethynylene derivative [10]. Among the various concepts for achieving a highly efficient photoinduced charge generation, one of the well-known routes is “the bulk heterojunction concept”, which uses acceptor materials with high electron affinity (such as C_{60} or soluble derivatives of C_{60}) mixed with conjugated polymers as electron donors [11a,b,c]. The behaviour of OFETs based on conjugated polymer/fullerene blends as active layers in FET configuration in the dark (including ambipolar transport) has been reported [12a,b,13]. However, photOFETs based on conjugated polymer/fullerene blends, which are expected to show higher photoresponsivity in comparison to devices with single components [7–10], have not been reported until now.

In this paper, we report on photOFETs based on conjugated polymer/fullerene blends as the photoactive semiconductor layer and poly-vinyl-alcohol (PVA) or divinyltetramethyldisiloxane-bis(benzocyclobutene) (BCB) as a highly transparent polymeric gate dielectrics. PhotOFETs fabricated on PVA show high responsivity but weak photostability, whereas photOFETs fabricated on BCB show transistor behaviour in a broad range of illumination intensities and good photostability even at high illumination. For devices with both dielectrics, the increase in drain–source current under illumination suggests the generation of carriers in the bulk of the highly photoactive conjugated polymer/fullerene blend. Interface charging effects, i.e. charge trapping at the interface between the dielectric and the bulk, resulting in hysteresis in transfer curves, is observed.

2. Experimental

A scheme of the device structure is presented in Fig. 1 together with the chemical structures of the materials used. PhotOFETs were fabricated on cleaned and patterned indium tin oxide (ITO) glass substrates. For PVA based devices, PVA with an average molecular weight of 127,000 (Sigma–Aldrich Mowiol® 40–88) was used as received. A pinhole free film of PVA gate dielectric was cast from a 10 wt.% aqueous solution by spin coating with 1500 rpm. From the thickness of the dielectric layer $d = 3.8 \mu\text{m}$ and the dielectric constant $\epsilon_{\text{PVA}} = 8$, a capacitance of $C_{\text{PVA}} = 1.8 \text{ nF/cm}^2$ is estimated. BCB precursor solution (used as received from Dow Chemicals) was spin coated at 1500 rpm resulting in a 2- μm thick pinhole free film. The cross-linking to BCB was done as described previously [6b,14,15]. BCB forms an inert dielectric layer with excellent mechanical properties and chemical stability, however with a rather low dielectric constant $\epsilon_{\text{BCB}} = 2.6$ ($C_{\text{BCB}} = 1.2 \text{ nF/cm}^2$). As photoactive material, a blend of MDMO-PPV (poly[2-methoxy-5-(3,7-dimethyloctyloxy)-1,4-phenylenevinylene] and (PCBM) methanofullerene [6,6]-phenyl C_{61} -butyric acid methyl ester (1: 4 wt. ratio) was spin coated at 1500 rpm from 0.5 wt.% chlorobenzene solution, yielding films around 170 nm, inside a glove box under argon atmosphere. The surface morphology and the thickness of the dielectric and the blend film were determined with a Digital Instrument 3100 atomic force microscope (AFM) and a Dektak surface profilometer. As top source and drain contacts, LiF/Al (0.6/60 nm) was evaporated under vacuum (5×10^{-6} mbar) through a shadow mask. The channel length, L , of all devices was 35 μm and the channel width, W , was 2 mm. All electrical characterisations were carried out under inert argon environment inside a glove box system or under vacuum. For the steady state current–voltage measurements, Keithley 2400 and Keithley 236 instruments were used. For the characterisation of the devices under illumination, a solar simulator (K.H. Steuernagel Lichttechnik GmbH) with intensities varying from 0.1 to 100 mW/cm^2 by using neutral density filters was used. The devices were illuminated through the ITO glass and the transparent dielectric layer as shown in Fig. 1(c).

3. Results and discussion

Output characteristics of a photOFET based on MDMO-PPV:PCBM (1:4) blends fabricated on

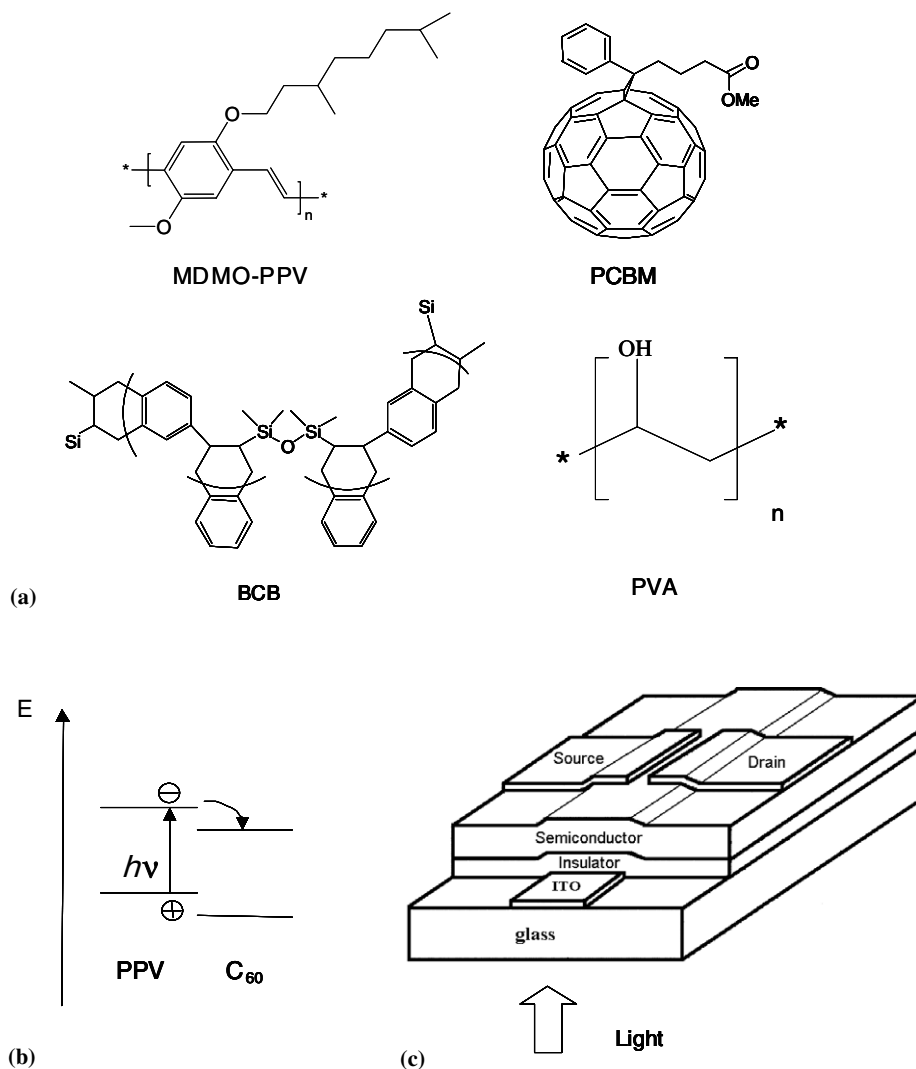


Fig. 1. (a) Molecular structure of MDMO-PPV, PCBM, BCB and PVA; (b) scheme of the photoinduced charge transfer between the PPV donor and the C₆₀ acceptor; (c) photOFET device structure.

top of the PVA gate-insulator with LiF/Al top source–drain contacts in dark are shown in Fig. 2(a). Electron accumulation mode is achieved with a positively biased gate voltage, V_{gs} , demonstrating n-type transistor behaviour, similar to the behaviour reported in pristine PCBM based devices [17]. It is assumed that LiF/Al forms ohmic contacts with the blend layer, especially with respect to charge injection and collection from the fullerene phase [16a,b,c]. Fig. 2(b) shows device transfer characteristics in dark (bottom curve). The calculated electron field-effect mobility, μ , was obtained from the saturation regime by using the following equation [18]:

$$I_{ds} = \frac{\mu WC_{PVA}}{2L} (V_{gs} - V_{th})^2, \quad (1)$$

where V_{th} is the threshold voltage, and found to be 10^{-2} cm²/V s. In pristine PCBM based OFETs, calculated electron mobilities as high as 0.2 cm²/V s have been observed [17], at least one order of magnitude higher than in the present blend devices. We presume that, in the blend, polymer chains significantly disturb the inter-molecular hopping transport in the fullerenes. A significant hysteresis in the dark transfer characteristics curve (Fig. 2(b)), when changing the sweep direction of the gate voltage, is observed. In other systems, the occurrence of a hysteresis has been attributed to charge trapping

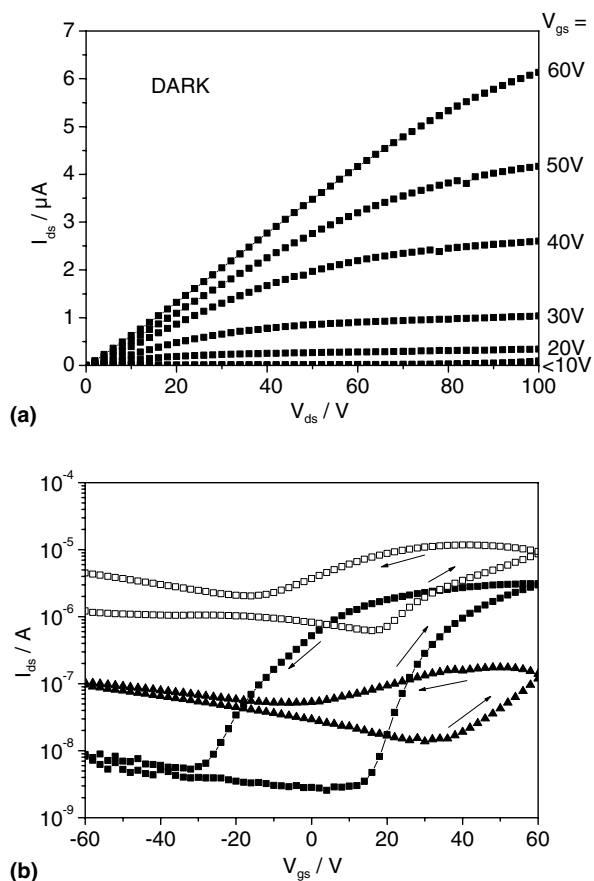


Fig. 2. (a) Output characteristics of the MDMO-PPV:PCBM (1:4) based photOFET fabricated on top of a PVA gate-insulator with LiF/Al as top source and drain electrodes in dark; (b) Transfer characteristics of the device in dark (filled square symbol curves), under AM1.5 (1 mW/cm^2) illumination (open square symbol curves) and in dark after illumination (filled triangular symbol curves) measured at $V_{ds} = +80 \text{ V}$. The arrows show the sweep directions.

effects at the semiconductor/dielectric interface or in the bulk of the dielectric [17,19,20]. Similar effects are expected to be the reason for the hysteresis in our devices as well.

The curves with open squares symbols (upper curve) in Fig. 2(b) show the photoresponse of the devices. At low white light (AM1.5) intensity of 1 mW/cm^2 , the transfer characteristics show gate voltage induced electron enhanced regime. In the depletion regime, I_{ds} increases more than two orders of magnitude in comparison to the currents in dark. The responsivity of the devices calculated (using Eq. (2)) from the depletion and the accumulation region, are 1.4 A/W and 5 A/W , respectively. At higher light intensities the drain–source current, I_{ds}

increases even more, becoming gate voltage independent and the device performance changes to a two terminal photoresistor.

The increase in I_{ds} can be explained by the generation of a large number of charge carriers due to the photoinduced charge transfer at the conjugated polymer/fullerene bulk heterojunction (photodoping). In contrast to expectations, still a high field is required for reaching the threshold voltage in the PVA based photOFET devices upon illumination, presumably due to complex interactions of different effects like charge trapping at the PVA/blend interface or in bulk of the dielectric or additional electric field induced charges. After switching off the light, a significant irreversible shift of the transfer curve in respect to the initial dark transfer characteristic was found (filled triangular symbol curves in Fig. 2(b)). We attribute that behaviour to photoinstability of the device. The origin and nature of the processes, which lead to photoinstability, are still under investigation.

In contrast to PVA, BCB as gate-insulator forms a much more photostable system. As mentioned above, cross-linked BCB forms an inert dielectric layer with excellent mechanical properties and chemical stability. On top of BCB, bulk heterojunction MDMO-PPV:PCBM (1:4) based photOFETs were fabricated. Electron enhanced mode in dark and under AM1.5 (100 mW/cm^2) illumination is achieved by biasing the devices with positive gate-source voltages, V_{gs} (Fig. 3(a)). The light response of the device is clearly observed by comparing the values of the drain–source current in dark and under illumination. Again, the increase of I_{ds} is caused by the creation of a large number of charge carriers due to photoinduced charge transfer between the conjugated polymer and the fullerene in the blend. A negligible hysteresis in the initial dark transfer characteristics is observed (filled squares symbol curves in Fig. 3(b)). A calculated electron mobility, μ_e of $10^{-2} \text{ cm}^2/\text{V s}$ is derived from the initial dark transfer characteristics at $V_{ds} = +80 \text{ V}$. The transfer characteristics of the device upon illumination with white light (AM1.5) and different illumination intensities (from 0.1 to 100 mW/cm^2) are shown in Fig. 3(b) with open symbol curves. The drain–source current of the device is significantly increased upon illumination, especially in the depletion regime. In the accumulation regime, the increase of the drain–source current is less pronounced.

The *responsivity*, R (expressed in A/W) of the device, can be defined as [8]:

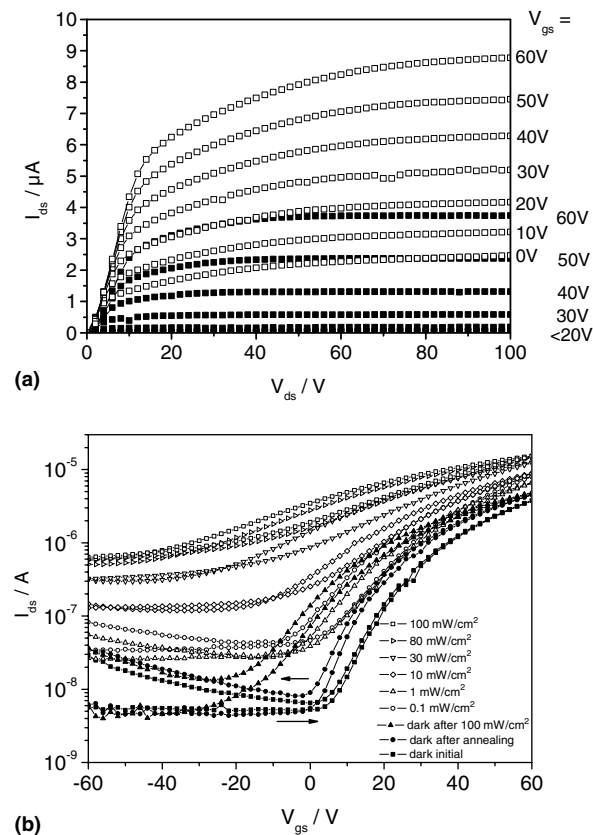


Fig. 3. (a) Output characteristics of the MDMO-PPV:PCBM (1:4) based photOFET fabricated on top of a BCB gate insulator with LiF/Al as top source and drain electrodes in dark (filled square symbol curves) and under AM1.5 (100 mW/cm²) (open square symbol curves); (b) transfer characteristics of the device in dark (filled square symbol curves), under AM1.5 illumination for different illumination intensities from 0.1 to 100 mW/cm² (open symbol curves), in dark after illumination (filled triangular symbol curves) and in dark after annealing at 130 °C for 3 min (filled circle symbol curves), measured at $V_{ds} = +80$ V. The arrows show the sweep directions.

$$R = \frac{I_{ph}}{P_{opt}} = \frac{(I_{ds,illum} - I_{ds,dark})S^{-1}}{P_{inc}}, \quad (2)$$

where I_{ph} is the drain–source photocurrent, P_{opt} is the incident optical power, P_{inc} the power of the incident light per unit area, $I_{ds,illum}$ the drain–source current under illumination, $I_{ds,dark}$ the drain–source current in the dark and S is the effective device area. The photOFET responsivity calculated from Eq. (2) in the depletion region was found to be 10 mA/W and in the accumulation regime was found to be 0.15 A/W, respectively. The threshold voltage for reaching the accumulation mode and opening of the transistor shifts to lower values upon illumination, suggesting that the trap carrier density in the channel is enhanced

by photodoping. The higher responsivity in the accumulation regime than in the depletion regime is attributed to the number of photogenerated charge carriers in the blend, which depends mostly on the light intensity and not on the applied gate voltage.

Upon illumination two different effects occur in the active layer of the transistor, i.e. *photoconductivity* and *photovoltaic effect*. When the transistor is in the ON-state the photocurrent is dominated by the photovoltaic effect and is given by Eq. (3) [21]:

$$I_{ph,pv} = G_M \Delta V_{th} = \frac{AkT}{q} \ln \left(1 + \frac{\eta q \lambda P_{opt}}{I_{pd} hc} \right), \quad (3)$$

where η is the quantum efficiency (i.e. number of carriers generated per photon), q is elementary charge, P_{opt} the incident optical power, I_{pd} the dark current for electrons, hc/λ the photon energy, G_M the transconductance, ΔV_{th} the threshold voltage shift, and A a fit parameter. The photovoltaic effect together with a shift of the threshold voltage is caused by the large number of trapped charge carriers under the source [7–10].

When the transistor is in the OFF-state, the photocurrent, dominated by photoconductivity is given by Eq. (4) [18]:

$$I_{ph,pc} = (q n E) W D = B P_{opt}, \quad (4)$$

where μ is the charge carrier mobility, n is the carrier density, E the electrical field in the channel, W the gate width, and D the thickness of the active layer. $I_{ph,pc}$ is therefore directly proportional to P_{opt} with a proportionality factor B . The experimental result of photOFETs based on MDMO-PPV:PCBM

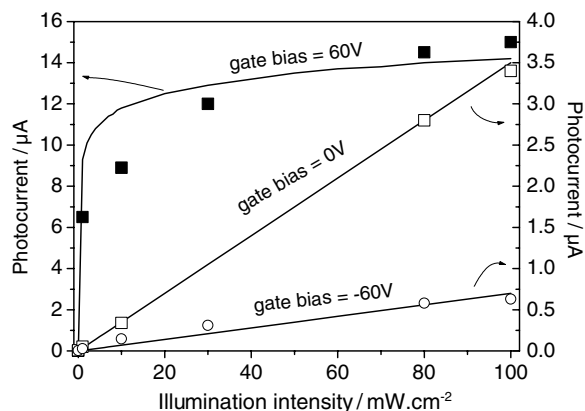


Fig. 4. Photocurrent as a function of illumination intensity in the ON-state ($V_{gs} = 60$ V, filled square symbols), under low gate bias ($V_{gs} = 0$ V, open square symbols) and in the OFF-state ($V_{gs} = -60$ V, open circle symbols). Solid lines are fits using Eqs. (3) and (4).

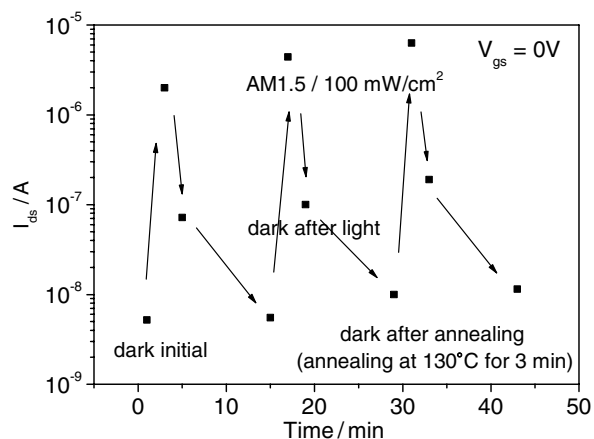


Fig. 5. Drain–source current for the MDMO-PPV:PCBM (1:4) photOFET recorded at $V_{gs} = 0$ V in the dark, under AM1.5 (100 mW/cm^2) illumination, again in the dark, and after annealing, for the first three cycles.

(1:4) blend as active layer and BCB as gate-insulator (Fig. 4) are in good agreement with the calculations.

After illumination, a shift in the dark transfer curve with respect to the initial dark transfer characteristics was observed (filled triangular symbol curves Fig. 3(b)) presumably due to the persistent interface effects, i.e. charge trapping, bias stressing, etc. [17,19,20,22]. In contrast to PVA, the initial dark can be recovered by annealing the device at 130°C for 3 min (filled circle symbol curves, Fig. 3(b)). Fig. 5 shows the drain–source current recorded sequentially at $V_{gs} = 0$ V in the dark, under AM1.5 (100 mW/cm^2) illumination, again in the dark and after annealing, for the first three cycles. The similar values for the respective dark/illumination situations show the good reversibility of the device. The existence of a state in the device with a larger current after illumination and prior to annealing may be considered as a memory state, which can be set by light and erased either by annealing or by applying a large negative gate voltage. It is proposed to exploit the effect of an increased dark state current after illumination in applications such as a light activated memory (“light memory device”).

4. Summary

In summary, we demonstrate photoresponsive OFETs (photOFET) based on MDMO-PPV:PCBM (1:4) blends with transparent insulating PVA or BCB layers as gate-dielectrics. The devices shown-type transistor characteristics with LiF/Al as top source

and drain electrodes. Devices fabricated with PVA as gate insulator show phototransistor behaviour at low light intensities with a high response. However, irreversibilities in the device properties after illumination occurred. PhotOFETs fabricated on top of cross-linked BCB as dielectric show phototransistor behaviour in a wide range of illumination intensities with sufficiently good photo-stability. The observation of an intermediate state (dark after illumination) has been proposed for use in “light memory devices”.

Acknowledgements

Special thanks are to G.J. Matt, A.J. Mozer, and A. Tanda for fruitful discussions. Financial support from the Austrian Foundation for the Advancement of Scientific Research (FWF P15629-N08) is gratefully acknowledged. S. Günes acknowledges the national award scholarship from Yildiz Technical University allocated from the Council of Higher Education of Turkey (YÖK).

References

- [1] H.E.A. Huitema, G.H. Gelinck, J.B.P.H. van der Putten, K.E. Kuijk, C.M. Hart, E. Cantatore, P.T. Herwig, A.J.J.M. van Breemen, D.M. de Leeuw, *Nature* 414 (2001) 599.
- [2] W. Clemens, W. Fix, J. Ficker, A. Knobloch, A. Ullmann, *J. Mater. Res.* 19 (2004) 1963.
- [3] B. Crone, A. Dodabalapur, A. Gelperin, L. Torsi, H.E. Katz, A.J. Lovinger, Z. Bao, *Appl. Phys. Lett.* 78 (2001) 2229.
- [4] A. Knobloch, A. Manuelli, A. Bernds, W. Clemens, *J. Appl. Phys.* 96 (2004) 2286.
- [5] (a) S.E. Shaheen, C.J. Brabec, N.N. Sariciftci, F. Padinger, T. Fromherz, J.C. Hummelen, *Appl. Phys. Lett.* 78 (2001) 841; (b) M.M. Wienk, J.M. Kroon, W.J.H. Varhees, J. Knol, J.C. Hummelen, P.A. Van Hal, R.A.J. Jansen, *Angew. Chem. Int. Ed.* 42 (2003) 3371.
- [6] (a) C.D. Dimitrakopoulos, P.R.L. Malenfant, *Adv. Mater.* 14 (2002) 99; (b) Th.B. Singh, N. Marjanović, G.J. Matt, S. Günes, N.S. Sariciftci, A.M. Ramil, A. Andreev, H. Sitter, R. Schwödiauer, S. Bauer, *Org. Electron.* 6 (2005) 105.
- [7] K.S. Narayan, N. Kumar, *Appl. Phys. Lett.* 79 (2001) 1891.
- [8] M.C. Hamilton, S. Martin, J. Kanicki, *IEEE Trans. Electron Dev.* 51 (2004) 877.
- [9] T.P.I. Saragi, R. Pudzych, T. Fuhrmann, J. Salbeck, *Appl. Phys. Lett.* 84 (2004) 2334.
- [10] Y. Xu, P.R. Berger, J.N. Wilson, U.H.F. Bunz, *Appl. Phys. Lett.* 85 (2004) 4219.
- [11] (a) N.S. Sariciftci, L. Smilowitz, A.J. Heeger, F. Wudl, *Science* 258 (1992) 1474; (b) C.H. Lee, G. Yu, D. Moses, K. Pakbaz, C. Zhang, N.S. Sariciftci, A.J. Heeger, F. Wudl, *Phys. Rev. B* 48 (1993) 15425; (c) C.J. Brabec, N.S. Sariciftci, J.C. Hummelen, *Adv. Func. Mater.* 11 (2001) 15.

- [12] (a) E.J. Meier, D.M. de Leeuw, S. Setayesh, E. van Veenendaal, B.-H. Huisman, P.W.M. Blom, J.C. Hummelen, U. Scherf, T.M. Klapwijk, *Nature Mater.* 2 (2003) 678;
(b) W. Geens, T. Martens, J. Poortmans, T. Aernouts, J. Manca, L. Lutsen, P. Heremans, S. Borghs, R. Mertens, D. Vanderzande, *Thin Solid Films* 451–452 (2004) 498.
- [13] Th.B. Singh, S. Günes, N. Marjanović, N.S. Sariciftci, R. Menon, *J. Appl. Phys.* 97 (2005) 114508.
- [14] L.-L. Chua, P.K.H. Ho, H. Sirringhaus, R.H. Friend, *Appl. Phys. Lett.* 84 (2004) 3400.
- [15] R. Schwödiauer, G.S. Neugschwandtner, S. Bauer-Gogonea, S. Bauer, W. Wirges, *Appl. Phys. Lett.* 75 (1999) 3998.
- [16] (a) V.D. Mihailetchi, J.K.J. van Duren, P.W.M. Blom, J.C. Hummelen, R.A.J. Janssen, J.M. Kroon, M.T. Rispens, W.J.H. Verhees, M.M. Wienk, *Adv. Func. Mater.* 13 (2003) 43;
(b) G.J. Matt, N.S. Sariciftci, T. Fromherz, *Appl. Phys. Lett.* 84 (2004) 1570;
(c) C.J. Brabec, A. Cravino, D. Meissner, N.S. Sariciftci, T. Fromherz, M.T. Rispens, L. Sanchez, J.C. Hummelen, *Adv. Funct. Mater.* 11 (2001) 374.
- [17] Th.B. Singh, N. Marjanović, P. Stadler, M. Auinger, G.J. Matt, S. Günes, N.S. Sariciftci, R. Schwödiauer, S. Bauer, *J. Appl. Phys.* 97 (2005) 083714.
- [18] S.M. Sze, *Physics of Semiconductor Devices*, Wiley, New York, 1981.
- [19] Th.B. Singh, N. Marjanović, G.J. Matt, N.S. Sariciftci, R. Schwödiauer, S. Bauer, *Appl. Phys. Lett.* 85 (2004) 5409.
- [20] L.-L. Chua, J. Zaumell, J.-F. Chang, E.C.-W. Ou, P.K.-H. Ho, H. Sirringhaus, R.H. Friend, *Nature* 434 (2005) 194.
- [21] H.-S. Kang, C.S. Choi, W.-Y. Choi, D.-H. Kim, K.-W. Seo, *Appl. Phys. Lett.* 84 (2004) 3780.
- [22] A. Salleo, M.L. Chabinyc, M.S. Yang, R.A. Street, *Appl. Phys. Lett.* 81 (2002) 4383.